A Substrate-Binding Metal-Organic Layer Selectively Catalyzes Photoredox Ene-Carbonyl Reductive Coupling Reactions

Yingjie Fan, Eric You, Ziwan Xu, and Wenbin Lin*

Department of Chemistry, The University of Chicago, Chicago, Illinois 60637, United States

ABSTRACT: Intermolecular photoredox ene-carbonyl reductive coupling reactions typically have low product selectivity owing to competing dimerization and/or reduction of ketyl radicals. Herein, we report a metal-organic layer (MOL), Hf-Ir-OTf, as a bifunctional photocatalyst for selective photoredox reductive coupling of ketones or aldehydes with electron-deficient alkenes. Composed of iridium-based photosensitizers (Ir-PSs) and triflated Hf_{12} clusters, Hf-Ir-OTf uses Lewis acidic Hf sites to bind and activate electron-deficient alkenes to accept ketyl radicals generated by adjacent Ir-PSs, thereby suppressing undesired dimerization and reduction of ketyl radicals to enhance the selectivity for the cross-coupling products. The MOL-catalyzed reductive coupling reaction accommodates a variety of olefinic substrates and tolerates reducible groups, nicely complementing current methods for cross-coupling reactions.

Photoredox reactions have provided powerful methods to generate and use radicals over the past decade.[1-3] For ene-carbonyl reductive coupling (ECRC) reactions, conventional methods rely on stoichiometric amounts of strong reductants, such as SmI_2,[4] Mg,[5] and Zn,[6] to generate ketyl radicals, which react with olefinic substrates to afford the coupling products. By using mild reductants such as Hantzsch ester to generate ketyl radicals, photoredox ECRC reactions increase functional group compatibility. The photoredox strategy has been successful in intramolecular addition of ketones to olefins[7] and imines[8] and coupling of alkenylpyridines[9-10] or allyl sulphones[11] with aldehydes and imines[9], as well as for some reactions under continuous flow conditions.[12] However, intermolecular photoredox ECRC reactions are not accessible for many olefin substrates due to competing pinacol coupling and/or reduction of ketones and aldehydes under these conditions, resulting in poor product selectivity.[9, 13]

Natural enzymes have provided a blueprint for tuning reaction selectivity by employing finely assembled pockets to specifically bind and activate substrates (Figure 1a).[14-15] A substrate selectively docks into the binding pocket to break and form bonds, and is then released from the active site, thereby preventing unwanted side reactions. This substrate-binding strategy has been demonstrated for a few homogeneous catalysts in selective alkane oxidation and C-H functionalization, but cannot be generalized to other organic reactions due to the difficulty of creating precise binding sites in molecular systems.[16-17]

Metal-organic layers (MOLs)[18-22], a dispersible monolayered-version of metal-organic frameworks (MOFs),[23-34] have shown great promise in synergistic catalysis by integrating multiple freely accessible catalytic centers.[35-39] In our previous work, MOLs combined photoredox and Lewis acid catalysts to increase the efficiency of dehydrogenative cross coupling reactions by facilitating electron and mass transfer.[40] We envision that the Lewis acidic groups in the MOL can act as an enzyme-mimicking substrate-binding site to enhance reaction selectivity by increasing the local concentration of a substrate and activating the substrate for addition to a transiently generated intermediate.

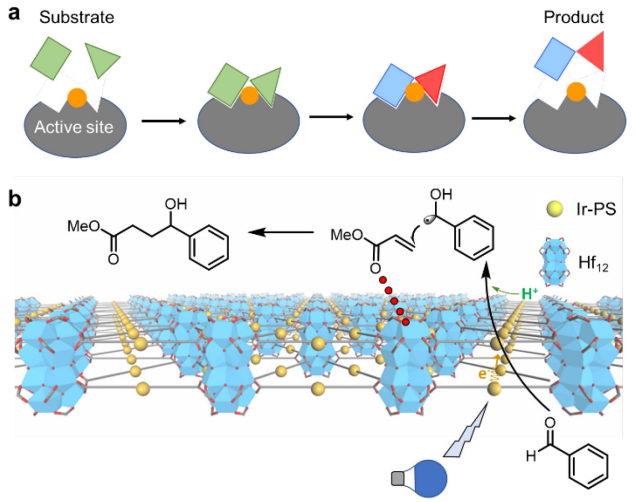

Figure 1. Schematics showing (a) substrate binding in enzyme catalysis and (b) Hf-Ir-OTf catalyzed photoredox ECRC reactions in which Hf_{12} clusters bind and activate olefins to facilitate addition of photo-generated ketyl radicals.

Herein, we report Hf-Ir-OTf MOL, consisting of triflate (OTf)-capped Hf_{12} SBUs and photosensitizing $[Ir(DBB)(dF(CF_3)ppy)_2]^+$ (Ir-PS; DBB = 4,4′-di(4-benzoato)-2,2′-bipyridine; dF-(CF_3)ppy = 2-(2,4-difluorophenyl)-5-(trifluoromethyl)-pyridine] ligands, as a selective catalyst for photoredox ECRC reactions. The triflated Hf_{12} clusters bind olefinic substrates via Lewis acid-base interaction to accelerate the addition of the ketyl radical generated by Ir-PS (Figure 1b). By depleting the ketyl radical, Hf-Ir-OTf minimizes ketyl dimerization and reduction reactions and increases the ECRC product yield by an order of magnitude over homogeneous controls.

Self-supporting MOL of the formula $Hf_{12}(\mu_3\text{-}O)_8(\mu_3\text{-}OH)_8(\mu_2\text{-}OH)_6(Ir\text{-}PS)_6(TFA)_6$ (Hf-Ir-TFA) was prepared by a solvothermal reaction between $HfCl_4$ and Ir-PS in dimethylformamide with water and trifluoroacetic acid (TFA) as modulators.[40] TFA capping groups were replaced with OTf groups via to produce $Hf_{12}(\mu_3\text{-}O)_8(\mu_3\text{-}OH)_8(\mu_2\text{-}OH)_6(Ir\text{-}PS)_6(OTf)_6$ (Hf-Ir-OTf, Figure S1, supporting information). Powder X-ray diffraction (PXRD) showed Hf-Ir-OTf retained the structure of Hf-Ir-TFA (Figure 2e). Transmission electron microscopy (TEM) and atomic force microscopy (AFM) revealed a monolayer hexagonal nanoplate morphology for Hf-Ir-OTf, with a diameter of approximately 300 nm and a thickness of approximately 1.8 nm (Figure 2b-d). Inductively coupled plasma-mass spectrometry (ICP-MS) confirmed a Hf to Ir ratio of 2:1 in both Hf-Ir-TFA and Hf-Ir-OTf, whereas nuclear magnetic resonance (NMR) spectra of digested MOLs supported their proposed formulae (Figure S3-S6, supporting information). In the structure of Hf-Ir-OTf, Hf_{12} clusters are laterally connected by Ir-PS ligands and vertically capped by OTf groups to afford strongly Lewis acidic Hf sites (Figure 2a).[40]

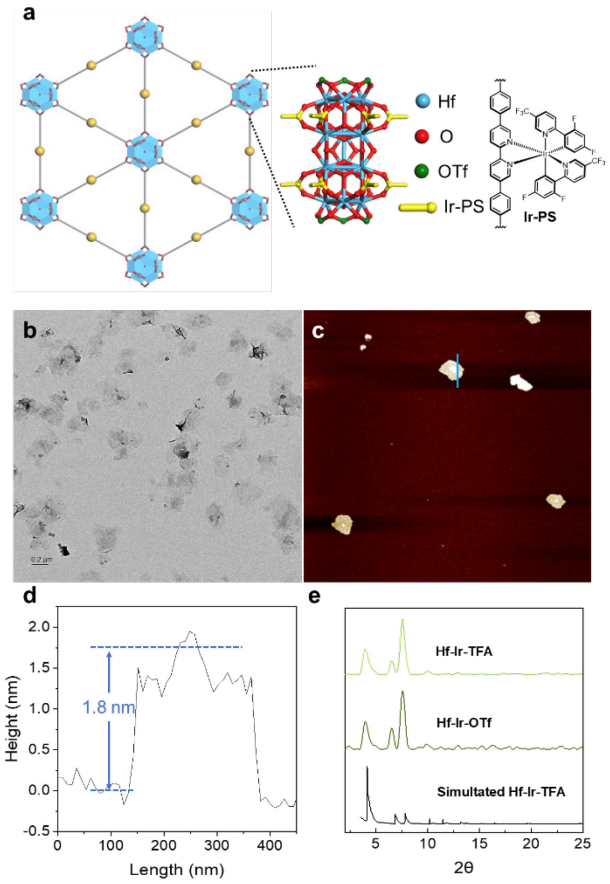

Figure 2. Structural model and characterization of Hf-Ir-OTf. (a) Schematic showing connectivity of Hf-Ir-OTf. (b-d) TEM image (b), AFM image (c), and height profile (d) of Hf-Ir-OTf. (e) PXRD patterns of Hf-Ir-TFA and Hf-Ir-OTf along with the simulated PXRD pattern of Hf-Ir-TFA.

Hf-Ir-OTf was examined as a photoredox catalyst for the coupling between 4-fluorobenzaldehyde (**1a**) and methyl acrylate (**1b**) (Table 1). At 0.05 mol% loading of Hf-Ir-OTf under blue LED irradiation, the ECRC product **1** was obtained in 91% yield with bis(2-methoxyethyl) 2,6-dimethyl-1,4-dihydropyridine-3,5-dicarboxylate (HEH) as reductant and 1,4-dioxane as solvent. In contrast, the reaction yielded alcohol (**1c**) only when 0.25 mol% Ir-PS methyl ester and 30 mol% $Sc(OTf)_3$ were used under otherwise identical conditions. When the loadings of both Ir-PS and $Sc(OTf)_3$ were reduced to 0.05 mol%, the yield of **1** increased to 52% but the dimerization byproduct **1d** was obtained in 48% yield. Combination of Ir-PS with other Lewis acids in different solvents did not improve the yield of **1** (Table S1, supporting information). Control reaction using Hf-Ir-OTf without light irradiation showed no product formation, indicating photocatalytic nature of the coupling reaction.

Table 1. Photoredox ECRC reactions catalyzed by Hf-Ir-OTf and homogeneous controls.

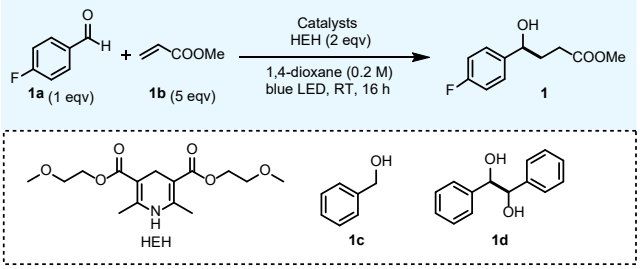

Entry	Catalyst(s)	Yield (**1**)[a]	Yield (**1c**)[a]	Yield (**1d**)[a]
1	0.05 mol% Hf-Ir-OTf	91%	0	9%
2	0.25 mol% Ir-PS, 30 mol% $Sc(OTf)_3$	0	>99%	0
3	0.05 mol% Ir-PS, 0.05 mol% $Sc(OTf)_3$	52%	0	48%
4	0.05 mol% Hf-Ir-OTf[b]	0	0	0

[a]Based on NMR analysis of the crude products. [b]Without blue LED irradiation.

To investigate the origin of product selectivity in Hf-Ir-OTf catalyzed reactions, we examined catalytic activities of Hf-Ir MOLs modified with Brønsted acids of varying pKa values: HOTf (-14.2),[41] $ClSO_3H$ (-6.0),[42], TFA (-0.3),[43] and AcOH (4.8).[43] Hf-Ir-OSO_2Cl and Hf-Ir-OAc were prepared from Hf-Ir-TFA by acid exchange and retained the structure and morphology of Hf-Ir-TFA (Figure S1, S2, supporting information). ICP-MS and NMR indicated complete exchange of TFA to OSO_2Cl and OAc capping groups, respectively, in Hf-Ir-OSO_2Cl and Hf-Ir-OAc. At 0.25 mol% catalyst loading, four Hf-Ir MOLs with different capping groups showed an increasing selectivity of **1** over **1d** as the pKa of the capping acid decreased (Table S1, supporting information), suggesting that the ECRC product selectivity increases as the binding of **1b** to the Hf site becomes stronger.[44-45]

Luminescence quenching studies (Figure S15) imply that the photoredox ECRC reaction starts with the quenching of photoexcited Ir-PS by HEH radical to generate highly reducing Ir(II) species.[9] According to previous reports,[9, 11] Ir(II) will transfer one electron to pyridinium activated **1a** to afford a ketyl radical, which then adds to Hf-bound **1b** to yield the coupling product **1**. However, the ketyl radicals also dimerize to yield the pinacol coupling product **1d.**[13] The product selectivity thus depends on relative rate of ketyl radical addition to **1b** and to another ketyl radical. It is likely that the Hf sites in Hf-Ir MOLs bind and activate **1b** for addition to the ketyl radical, thereby increasing the selectivity for **1**.

To support this hypothesis, we performed kinetic experiments targeting products **1** and **1d** using 0.05 mol% loading of four Hf-Ir MOLs with different capping groups and four different loadings of Hf-Ir-OTf (0.05, 0.10, 0.25, and 0.50 mol%). We approximated the ratios of product yields for **1**/**1d** in the first 5 min for different loadings of Hf-Ir-OTf and in the first 10 min for Hf-Ir MOLs with different capping groups as the ratios of initial product formation rates of **1** over **1d** (Figure 3a, 3b). The selectivity **1**/**1d** was negatively corelated to both pKa values of capping acids and catalyst loadings. The negative correlation of **1**/**1d** selectivity to capping acid pKa suggests that the Hf sites act as Lewis acids to bind and activate electron-deficient olefins and Hf sites with stronger capping acids render the bound substrate more electron-deficient to facilitate radical addition to the olefin. The negative correlation of **1**/**1d** selectivity to Hf-Ir-OTf loading can be explained by different reaction orders of ECRC (1st order) and pinacol dimerization (2nd order) reactions on the ketyl radicals. Higher Ir-PS concentration increases the concentration of photo-generated ketyl radicals, thus promoting the undesired pinacol dimerization reaction (see supporting information S4.3 for detailed analysis).

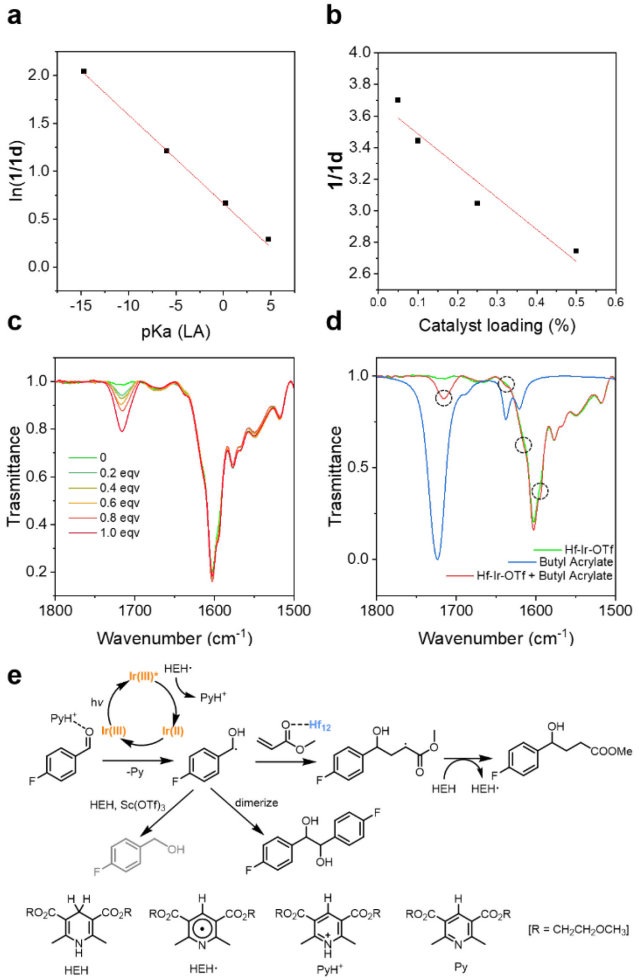

Figure 3. Mechanistic studies of Hf-Ir-OTf catalyzed ECRC reactions. (a,b) Plots of reaction selectivity versus capping acid pKa (a) and Hf-Ir-OTf loading (b). (c) IR spectra of Hf-Ir-OTf with different equivalents of butyl acrylate. (d) IR spectra of butyl acrylate, Hf-Ir-OTf, and Hf-Ir-OTf mixed with 1 equiv of butyl acrylate. Characteristic peaks of butyl acrylate in the mixture IR spectrum are highlighted by black circles. (e) Proposed mechanism of Hf-Ir-OTf catalyzed ECRC reaction.

The interaction between Hf-Ir-OTf and olefinic substrates was examined by infrared (IR) spectroscopy and diffusion-ordered spectroscopy (DOSY). IR spectra of Hf-Ir-OTf with different equivalents of butyl acrylate were collected (Figure 3c). The addition of butyl acrylate generated four peaks at around 1715, 1638, 1617 and 1594 cm^{-1} (Figure 3d), which were assigned to free carbonyl, *trans*-C=C bond, *cis*-C=C bond, and bound carbonyl stretching vibrations from butyl acrylate, respectively.[46-47] The peak intensity at 1594 cm^{-1} increases with addition of more butyl acrylate in the different spectra (Figure S13, supporting information), supporting the peak assignments. A red shift of 121 cm^{-1} in carbonyl vibrations indicated that the carbonyl group in acrylate was strongly activated when bound to Hf-Ir-OTf. On the other hand, DOSY showed a decrease of diffusion constant of **1b** in solution after Hf-Ir-OTf was added (Figure S11, S12, supporting information). Specifically, the diffusion constant of **1b** decreased from 3.9×10^{-5} cm^2/s to 3.3×10^{-5} cm^2/s methyl proton at 3.7 ppm, indicating strong interaction between Hf-Ir-OTf and **1b**.[48-50]

On the basis of these experimental results and literature precedents,[9] we propose the following mechanism for Hf-Ir-OTf catalyzed photoredox ECRC reactions (Figure 3e). The reaction starts with a photoredox cycle reducing an aldehyde to a ketyl radical. The reactive ketyl radical preferably attacks C=C double bond in Hf-bound **1b**. The resultant α-carbonyl radical then abstracts a hydrogen from HEH to afford **1**. In the meantime, the ketyl radical can dimerize to form the pinacol coupling product **1d** or abstract a hydrogen atom to afford the benzyl alcohol product **1c** in the presence of high loadings of Lewis acids. This mechanistic scenario explains the higher reductive coupling selectivity of Hf-Ir-OTf over homogeneous catalysts: Lewis acidic Hf sites bind the olefinic substrate to increase its local concentration and to make it more electron-deficient for coupling with the ketyl radical. The lower loadings of Lewis acids in Hf-Ir-OTf catalyzed reactions also help to suppress the formation of **1c**.

The substrate scope of Hf-Ir-OTf catalyzed ECRC reactions was explored at 0.05 mol% catalyst loading (Table 2). Aromatic aldehydes with halo (**1a**, **4a**, **5a**), aryl (**3a**), and cyano (**7a**) substituents all underwent ECRC reactions to afford desired products **1**, **3**, **4**, **5**, and **7** in 78-93% yields. Aromatic aldehydes with electron-donating methoxy and dimethylamino groups (**2a**, **8a**) underwent ECRC reactions to afford **2** and **8** in slightly lower yields of 81% and 61%. Extending reaction time from 16 h to 48 h increased the yield of **8** from 61% to 82%. Reactions with pyridine- and furan-substituted aldehydes **6a** and **9a** afforded corresponding coupling product in 81% and 56% yields, respectively. Ketones **10a** and **11a** also reacted with acrylate to afford tertiary alcohols **10** and **11** in 41% and 58% yields, respectively. The lower reactivity of ketones is likely a result of their less efficient reduction to ketyl radicals. Olefinic substrates with several different electron-withdrawing groups, including cyano, carboxylic esters, pyridine, phosphate, and sulfonate groups also coupled with **1a** to afford coupling products **12-14, 16-18** in 56-92% yields. Reaction between **1a** and α-substituted acrylate **15b** afforded diastereomers of **15** in 65% yield. Finally, terminal and internal alkynes with carboxylate ester groups also reacted with **1a** to generate di-substituted or tri-substituted olefins (**19** or **20**) in ~60% yields. The broad scopes of both carbonyl and olefin substrates of the ECRC reactions indicate the generality of this substrate-binding strategy. Hf-Ir-OTf was

reused for at least four times without loss of catalytic activity (Figure S10, supporting information). The present photoredox ECRC reaction complements current methods for ECRC reactions by accommodating a variety of acrylate substrates and tolerating reducible groups.

Table 2. Substrate scope of Hf-Ir-OTf catalyzed photoredox ECRC reactions.

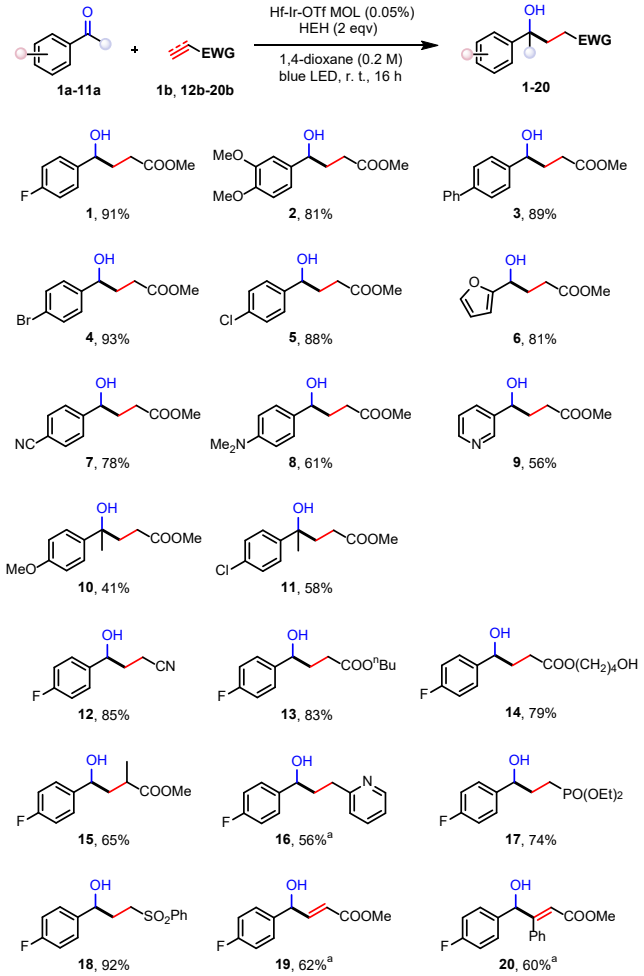

[a]Reactions are performed in dichloromethane.

In summary, we have developed a substrate-binding MOL as a photoredox catalyst for selective ECRC reactions. In the coupling between 4-fluorobenzaldehyde and methyl acrylate, Hf-Ir-OTf increased the selectivity for the ECRC product by an order of magnitude over homogeneous controls. Spectroscopic and kinetic studies revealed Lewis acids in Hf-Ir-OTf bind and activate olefinic substrates to facilitate addition to photo-generated ketyl radicals. MOL-catalyzed ECRC reaction has good functional group tolerance and accommodates various acrylate substrates and aromatic carbonyl compounds. Hierarchical integration of both Lewis acids and photosensitizers in Hf-Ir-OTf thus enables the unique catalytic activity for selective ECRC reactions. MOLs promise to serve as an excellent platform for developing new generation of multifunctional materials with biomimetic catalytic activities.

ASSOCIATED CONTENT

The supporting information is available free of charge on the ACS Publication website at

Synthesis and characterization of Hf-Ir MOLs, catalytic reactions, and mechanistic studies.

AUTHOR INFORMATION

Corresponding Author

Wenbin Lin − *Department of Chemistry, The University of Chicago, Chicago, Illinois 60637, United States*; orcid.org/0000-0001-7035-7759;
Email: wenbinlin@uchicago.edu

Other Authors

Yingjie Fan − *The University of Chicago, Chicago, Illinois 60637, United States*
Eric You − *The University of Chicago, Chicago, Illinois 60637, United States*
Ziwan Xu − *The University of Chicago, Chicago, Illinois 60637, United States*; http://orcid.org/0000-0001-9459-4572

Author Contributions

The manuscript was written through contributions of all authors.

Notes

The authors declare no competing financial interest.

ACKNOWLEDGMENT

We thank Xiaomin Jiang and Yang Song for experimental help and Dr. Josh Kurutz for help with diffusion-ordered spectroscopy. We acknowledge the National Science Foundation (CHE-2102554) and the University of Chicago for funding support and the MRSEC Shared User Facilities at the University of Chicago (DMR-1420709) for instrument Access.

REFERENCES

1. Romero, N. A.; Nicewicz, D. A., Organic Photoredox Catalysis. *Chemical Reviews* **2016,** *116* (17), 10075-10166.
2. Twilton, J.; Le, C.; Zhang, P.; Shaw, M. H.; Evans, R. W.; MacMillan, D. W. C., The merger of transition metal and photocatalysis. *Nature Reviews Chemistry* **2017,** *1* (7), 0052.
3. Matsui, J. K.; Lang, S. B.; Heitz, D. R.; Molander, G. A., Photoredox-Mediated Routes to Radicals: The Value of Catalytic Radical Generation in Synthetic Methods Development. *ACS Catalysis* **2017,** *7* (4), 2563-2575.
4. Fukuzawa, S.-i.; Nakanishi, A.; Fujinami, T.; Sakai, S., Reductive coupling of ketones or aldehydes with electron-deficient alkenes promoted by samarium di-iodide. *Journal of the Chemical Society, Chemical Communications* **1986,** (8), 624-625.
5. Pons, J.-M.; Santelli, M., Conjugate addition of the dianion of diaryl ketones to α, β- ethylenic ketones promoted by TiCl4-Mg. *Tetrahedron* **1990,** *46* (2), 513-522.
6. Yeh, C.-H.; Korivi, R. P.; Cheng, C.-H., Ene-Carbonyl Reductive Coupling Mediated by Zinc and Ammonia for the Synthesis of γ-Hydroxybutyric Acid Derivatives. *Advanced Synthesis & Catalysis* **2013,** *355* (7), 1338-1344.
7. Tarantino, K. T.; Liu, P.; Knowles, R. R., Catalytic Ketyl-Olefin Cyclizations Enabled by Proton-Coupled Electron Transfer. *Journal of the American Chemical Society* **2013,** *135* (27), 10022-10025.
8. Rono, L. J.; Yayla, H. G.; Wang, D. Y.; Armstrong, M. F.; Knowles, R. R., Enantioselective Photoredox Catalysis Enabled by Proton-Coupled Electron Transfer: Development of an Asymmetric Aza-Pinacol Cyclization. *Journal of the American Chemical Society* **2013,** *135* (47), 17735-17738.
9. Lee, K. N.; Lei, Z.; Ngai, M.-Y., β-Selective Reductive Coupling of Alkenylpyridines with Aldehydes and Imines via Synergistic Lewis Acid/Photoredox Catalysis. *Journal of the American Chemical Society* **2017,** *139* (14), 5003-5006.
10. Cao, K.; Tan, S. M.; Lee, R.; Yang, S.; Jia, H.; Zhao, X.; Qiao, B.; Jiang, Z., Catalytic Enantioselective Addition of Prochiral

Radicals to Vinylpyridines. *Journal of the American Chemical Society* **2019,** *141* (13), 5437-5443.

11. Qi, L.; Chen, Y., Polarity-Reversed Allylations of Aldehydes, Ketones, and Imines Enabled by Hantzsch Ester in Photoredox Catalysis. *Angewandte Chemie International Edition* **2016,** *55* (42), 13312-13315.

12. Seo, H.; Jamison, T. F., Catalytic Generation and Use of Ketyl Radical from Unactivated Aliphatic Carbonyl Compounds. *Organic Letters* **2019,** *21* (24), 10159-10163.

13. Nakajima, M.; Fava, E.; Loescher, S.; Jiang, Z.; Rueping, M., Photoredox-Catalyzed Reductive Coupling of Aldehydes, Ketones, and Imines with Visible Light. *Angewandte Chemie International Edition* **2015,** *54* (30), 8828-8832.

14. Koshland, D. E., Application of a Theory of Enzyme Specificity to Protein Synthesis. *Proceedings of the National Academy of Sciences* **1958,** *44* (2), 98.

15. Sullivan, S. M.; Holyoak, T., Enzymes with lid-gated active sites must operate by an induced fit mechanism instead of conformational selection. *Proceedings of the National Academy of Sciences* **2008,** *105* (37), 13829.

16. Das, S.; Incarvito, C. D.; Crabtree, R. H.; Brudvig, G. W., Molecular Recognition in the Selective Oxygenation of Saturated C-H Bonds by a Dimanganese Catalyst. *Science* **2006,** *312* (5782), 1941.

17. Engle, K. M.; Mei, T.-S.; Wasa, M.; Yu, J.-Q., Weak Coordination as a Powerful Means for Developing Broadly Useful C–H Functionalization Reactions. *Accounts of Chemical Research* **2012,** *45* (6), 788-802.

18. Xue, Y.; Zhao, G.; Yang, R.; Chu, F.; Chen, J.; Wang, L.; Huang, X., 2D metal–organic framework-based materials for electrocatalytic, photocatalytic and thermocatalytic applications. *Nanoscale* **2021,** *13* (7), 3911-3936.

19. Jiang, Z. W.; Zou, Y. C.; Zhao, T. T.; Zhen, S. J.; Li, Y. F.; Huang, C. Z., Controllable Synthesis of Porphyrin-Based 2D Lanthanide Metal–Organic Frameworks with Thickness- and Metal-Node-Dependent Photocatalytic Performance. *Angewandte Chemie International Edition* **2020,** *59* (8), 3300-3306.

20. Cao, L.; Lin, Z.; Peng, F.; Wang, W.; Huang, R.; Wang, C.; Yan, J.; Liang, J.; Zhang, Z.; Zhang, T.; Long, L.; Sun, J.; Lin, W., Self-Supporting Metal–Organic Layers as Single-Site Solid Catalysts. *Angewandte Chemie International Edition* **2016,** *55* (16), 4962-4966.

21. Zhao, M.; Huang, Y.; Peng, Y.; Huang, Z.; Ma, Q.; Zhang, H., Two-dimensional metal–organic framework nanosheets: synthesis and applications. *Chemical Society Reviews* **2018,** *47* (16), 6267-6295.

22. Jian, M.; Qiu, R.; Xia, Y.; Lu, J.; Chen, Y.; Gu, Q.; Liu, R.; Hu, C.; Qu, J.; Wang, H.; Zhang, X., Ultrathin water-stable metal-organic framework membranes for ion separation. *Science Advances* **2020,** *6* (23), eaay3998.

23. Furukawa, H.; Cordova, K. E.; O'Keeffe, M.; Yaghi, O. M., The Chemistry and Applications of Metal-Organic Frameworks. *Science* **2013,** *341* (6149), 1230444.

24. Huang, Y.-B.; Liang, J.; Wang, X.-S.; Cao, R., Multifunctional metal–organic framework catalysts: synergistic catalysis and tandem reactions. *Chemical Society Reviews* **2017,** *46* (1), 126-157.

25. McDonald, T. M.; Mason, J. A.; Kong, X.; Bloch, E. D.; Gygi, D.; Dani, A.; Crocellà, V.; Giordanino, F.; Odoh, S. O.; Drisdell, W. S.; Vlaisavljevich, B.; Dzubak, A. L.; Poloni, R.; Schnell, S. K.; Planas, N.; Lee, K.; Pascal, T.; Wan, L. F.; Prendergast, D.; Neaton, J. B.; Smit, B.; Kortright, J. B.; Gagliardi, L.; Bordiga, S.; Reimer, J. A.; Long, J. R., Cooperative insertion of CO2 in diamine-appended metal-organic frameworks. *Nature* **2015,** *519* (7543), 303-308.

26. Yang, D.; Gates, B. C., Elucidating and Tuning Catalytic Sites on Zirconium- and Aluminum-Containing Nodes of Stable Metal–Organic Frameworks. *Accounts of Chemical Research* **2021,** *54* (8), 1982-1991.

27. Lee, J.; Farha, O. K.; Roberts, J.; Scheidt, K. A.; Nguyen, S. T.; Hupp, J. T., Metal–organic framework materials as catalysts. *Chemical Society Reviews* **2009,** *38* (5), 1450-1459.

28. Liu, J.; Chen, L.; Cui, H.; Zhang, J.; Zhang, L.; Su, C.-Y., Applications of metal–organic frameworks in heterogeneous supramolecular catalysis. *Chemical Society Reviews* **2014,** *43* (16), 6011-6061.

29. Bour, J. R.; Wright, A. M.; He, X.; Dincă, M., Bioinspired chemistry at MOF secondary building units. *Chemical Science* **2020,** *11* (7), 1728-1737.

30. Long, J. R.; Yaghi, O. M., The pervasive chemistry of metal–organic frameworks. *Chemical Society Reviews* **2009,** *38* (5), 1213-1214.

31. Li, H.; Eddaoudi, M.; O'Keeffe, M.; Yaghi, O. M., Design and synthesis of an exceptionally stable and highly porous metal-organic framework. *Nature* **1999,** *402* (6759), 276-279.

32. Wang, H.; Zhu, Q.-L.; Zou, R.; Xu, Q., Metal-Organic Frameworks for Energy Applications. *Chem* **2017,** *2* (1), 52-80.

33. Yang, D.; Odoh, S. O.; Borycz, J.; Wang, T. C.; Farha, O. K.; Hupp, J. T.; Cramer, C. J.; Gagliardi, L.; Gates, B. C., Tuning Zr6 Metal–Organic Framework (MOF) Nodes as Catalyst Supports: Site Densities and Electron-Donor Properties Influence Molecular Iridium Complexes as Ethylene Conversion Catalysts. *ACS Catalysis* **2016,** *6* (1), 235-247.

34. Cui, Y.; Yue, Y.; Qian, G.; Chen, B., Luminescent Functional Metal–Organic Frameworks. *Chemical Reviews* **2012,** *112* (2), 1126-1162.

35. Dhakshinamoorthy, A.; Asiri, A. M.; Garcia, H., 2D Metal–Organic Frameworks as Multifunctional Materials in Heterogeneous Catalysis and Electro/Photocatalysis. *Advanced Materials* **2019,** *31* (41), 1900617.

36. Lan, G.; Quan, Y.; Wang, M.; Nash, G. T.; You, E.; Song, Y.; Veroneau, S. S.; Jiang, X.; Lin, W., Metal–Organic Layers as Multifunctional Two-Dimensional Nanomaterials for Enhanced Photoredox Catalysis. *Journal of the American Chemical Society* **2019,** *141* (40), 15767-15772.

37. Quan, Y.; Lan, G.; Shi, W.; Xu, Z.; Fan, Y.; You, E.; Jiang, X.; Cheng, W.; Lin, W., Metal–Organic Layers Hierarchically Integrate Three Synergistic Active Sites for Tandem Catalysis. *Angewandte Chemie International Edition* **2020,** *133* (6), 3152-3157.

38. Guo, Y.; Wang, Y.; Shen, Y.; Cai, Z.; Li, Z.; Liu, J.; Chen, J.; Xiao, C.; Liu, H.; Lin, W.; Wang, C., Tunable Cobalt-Polypyridyl Catalysts Supported on Metal–Organic Layers for Electrochemical CO2 Reduction at Low Overpotentials. *Journal of the American Chemical Society* **2020,** *142* (51), 21493-21501.

39. Shi, W.; Cao, L.; Zhang, H.; Zhou, X.; An, B.; Lin, Z.; Dai, R.; Li, J.; Wang, C.; Lin, W., Surface Modification of Two-Dimensional Metal–Organic Layers Creates Biomimetic Catalytic Microenvironments for Selective Oxidation. *Angewandte Chemie International Edition* **2017,** *56* (33), 9704-9709.

40. Quan, Y.; Lan, G.; Fan, Y.; Shi, W.; You, E.; Lin, W., Metal–Organic Layers for Synergistic Lewis Acid and Photoredox Catalysis. *Journal of the American Chemical Society* **2020,** *142* (4), 1746-1751.

41. Trummal, A.; Lipping, L.; Kaljurand, I.; Koppel, I. A.; Leito, I., Acidity of Strong Acids in Water and Dimethyl Sulfoxide. *The Journal of Physical Chemistry A* **2016,** *120* (20), 3663-3669.

42. Guthrie, J. P., Hydrolysis of esters of oxy acids: pKa values for strong acids; Brønsted relationship for attack of water at methyl; free energies of hydrolysis of esters of oxy acids; and a linear relationship between free energy of hydrolysis and pKa holding over a range of 20 pK units. *100 Years of CSC in the Pages of CJC* **2011,** *01* (01), 2342-2354.

43. America Chemistry Society, Division of Organic Chemistry. *A pKa values in DMSO compitation (by Reich and Bordwell)*. American Chemical Society, 2021 https://organicchemistrydata.org/hansreich/resources/pka/pka_data/pka-compilation-reich-bordwell.pdf (accessed 2021-06-02).

44. Vermoortele, F.; Vandichel, M.; Van de Voorde, B.; Ameloot, R.; Waroquier, M.; Van Speybroeck, V.; De Vos, D. E., Electronic Effects of Linker Substitution on Lewis Acid Catalysis with Metal–Organic Frameworks. *Angewandte Chemie International Edition* **2012,** *51* (20), 4887-4890.

45. Ji, P.; Drake, T.; Murakami, A.; Oliveres, P.; Skone, J. H.; Lin, W., Tuning Lewis Acidity of Metal–Organic Frameworks via Perfluorination of Bridging Ligands: Spectroscopic, Theoretical, and

Catalytic Studies. *Journal of the American Chemical Society* **2018,** *140* (33), 10553-10561.

46. pp Coblentz Society, Inc., 'Evaluated Infrared Reference Spectra' in NIST Chemistry Webbook, NIST Standard Reference Database Number 69, National Institute of Standars and Technology, https://webbook.nist.gov/cgi/cbook.cgi?ID=C141322&Type=IR-SPEC&Index=1#IR-SPEC (retrieved June 8, 2021).

47. Hanson, C. S.; Psaltakis, M. C.; Cortes, J. J.; Siddiqi, S. S.; Devery, J. J., Investigation of Lewis Acid-Carbonyl Solution Interactions via Infrared-Monitored Titration. *The Journal of Organic Chemistry* **2020,** *85* (2), 820-832.

48. Shastry, T. A.; Morris-Cohen, A. J.; Weiss, E. A.; Hersam, M. C., Probing Carbon Nanotube–Surfactant Interactions with Two-Dimensional DOSY NMR. *Journal of the American Chemical Society* **2013,** *135* (18), 6750-6753.

49. Hens, Z.; Moreels, I.; Martins, J. C., In Situ 1H NMR Study on the Trioctylphosphine Oxide Capping of Colloidal InP Nanocrystals. *ChemPhysChem* **2005,** *6* (12), 2578-2584.

50. Fritzinger, B.; Moreels, I.; Lommens, P.; Koole, R.; Hens, Z.; Martins, J. C., In Situ Observation of Rapid Ligand Exchange in Colloidal Nanocrystal Suspensions Using Transfer NOE Nuclear Magnetic Resonance Spectroscopy. *Journal of the American Chemical Society* **2009,** *131* (8), 3024-3032.

TOC Graphic: